Article

Incisive Structure–Spectroscopic Correlation in Oligothiophenes Functionalized with (±) Inductive/Mesomeric Fluorine Groups: Joint Raman and DFT Study

Juan Casado, Vctor Hernndez, Mara C. Ruiz Delgado, Roco P. Ortiz, Juan T. Lpez Navarrete, Antonio Facchetti, and Tobin J. Marks

J. Am. Chem. Soc., **2005**, 127 (38), 13364-13372• DOI: 10.1021/ja053296n • Publication Date (Web): 02 September 2005

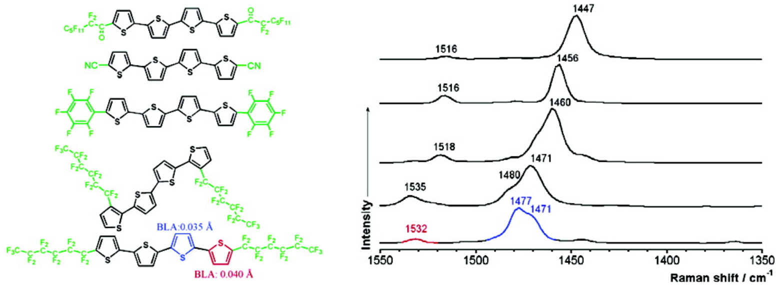

Journal of the American Chemical Society is published by the American Chemical Society. 1155 Sixteenth Street N.W., Washington, DC 20036

J|A|C|S
ARTICLES

Incisive Structure−Spectroscopic Correlation in Oligothiophenes Functionalized with (±) Inductive/Mesomeric Fluorine Groups: Joint Raman and DFT Study

Juan Casado,[†] Víctor Hernández,[†] María C. Ruiz Delgado,[†] Rocío P. Ortiz,[†]
Juan T. López Navarrete,*[,†] Antonio Facchetti,[‡] and Tobin J. Marks[‡]

Contribution from the Department of Physical Chemistry, University of Málaga, Campus de Teatinos s/n, Málaga 29071, Spain, and Department of Chemistry, Northwestern University, 2145 Sheridan Road, Evanston, Illinois 60208-3113

Received May 20, 2005; E-mail: teodomiro@uma.es.

Abstract: This paper presents a combined experimental Raman and density functional theory (DFT) study of a series of oligothiophenes with variable π−core lengths and substituted at the α,ω- and β,β'-terminal positions with perfluorohexyl, perfluorohexylcarbonyl, perfluoroarene, and cyano groups. The study covers the neutral and the electrochemically oxidized samples. The spectra have been assigned with the help of B3LYP/6-31G** calculations and interpreted by the predictions of effective conjugation coordinate (ECC) theory. Direct relationships between the bond length alternation (BLA) parameters and the Raman wavenumbers of the two most important bands of the spectra have been outlined showing the collective character of their electronic and vibrational properties. It is found that the topology of the thienyl electronic structure is not uniform along the conjugated core with the external rings more aromatic, whereas for the innermost part the π-electron delocalization is greater and extends with the increment of chain length. Perfluorohexyl substitution finely tunes the electronic properties via negative inductive effects. The β,β' isomers exhibit larger conformational distortion, which strongly modifies the mean conjugation length. Oxidation provokes electronic structure quinoidization spreading over the whole system but more marked in the central part of the π−core. The Raman features associated to quinoidization in the oxidized species have been interpreted in relation to the oligomer core length and the substitution regiochemistry.

I. Introduction

Over the past decade considerable effort has been focused on the synthesis of organic π-conjugated systems acting as semiconducting elements for electronics and optoelectronic applications, mainly field-effect transistors (OFETs), photovoltaics, and light-emitting diodes (OLEDs).[1,2] In addition to the success of the pentacene derivatives class,[2] one of the most fruitful studied groups of molecules are oligothiophenes due to, among many other reasons, their great chemical stability and facile functionalization combined with their excellent electronic properties, good thin film properties, etc. Oligothiophenes are intrinsically electron-rich systems, and consequently, they exhibit very good hole-transporting properties when implemented into FET devices. A number of studies are found in the literature dealing with improvement of the hole-transporting behavior of sexithiophene[3] (the prototypical compound), mainly through functionalization at the α,ω-positions with methyl,[4] ethyl, *n*-hexylthio,[5] or *n*-hexyl[6] groups in increasing degree of effectiveness.

However, to achieve a complete implementation in circuit architectures, these systems are required to behave also as electron-transporting materials. If this is achieved, oligothiophenes could act as ambipolar materials forming p−n junctions and complementary FET, which are the key features of conventional inorganic semiconductors (i.e., Si or Ge). This desirable ambipolar behavior has been achieved in a quinoid oligothiophene, 3′,4′-dibutyl-5,5″-bis(dicyanomethylene) -5,5″-dihydro-2,2′:5′,2″-terthiophene (TCN-3Q), which shows very

---

[†] University of Málaga.

[‡] Northwestern University.

(1) Shirakawa, H. *Chem. Commun*. **2003**, 1. Dimitrakopoulos, C. D.; Malenfant, P. R. L. *Adv. Mater*. **2002**, *14*, 99. Katz, H. E.; Bao, Z.; Gilat, S. L. *Acc. Chem. Res*. **2001**, *34*, 359. Crone, B.; Dodabalapur, A.; Llin, Y.-Y.; Filas, R. W.; Bao, Z.; LaDuca, A.; Sarpeshkar, R.; Katz, H. E. *Nature* **2000**, *403*, 521.

(2) Tour, J. M. *Acc. Chem. Res*. **2000**, *33*, 791. Pasini, M.; Destri, S.; Porzio, W.; Botta, C.; Giovanella, U. *J. Mater. Chem*. **2003**, *13*, 807. Suzuki, M.; Fukuyama, M.; Hori, Y.; Hotta, S. *J. Appl. Phys*. **2002**, *91*, 5706. Horowitz, G. *Adv. Mater*. **1998**, *10*, 365. Katz, H. E.; Lovinger, A. J.: Johnson, J.; Kloc, C.; Siegrist, T.; Li, W.; Linn, Y. Y.; Dobadalapur, A. *Nature* **2000**, *404*, 478. Bao, Z.; Rogers, J. A.; Katz, H. E. *J. Mater. Chem*. **1999**, *9*, 1895. Li, X. C.; Sirringhaus, H.; Garnier, F.; Holmes, A. B.; Moratti, S. C.; Feeder, N.; Clegg, W.; Teat, S. J.; Friend, R. H. *J. Am. Chem. Soc*. **1998**, *120*, 2206. Meng, H.; Bao, Z.; Lovinger, A. J.; Wang, B.; Mujsce, A. M. *J. Am. Chem. Soc*. **2001**, *123*, 9214.

(3) Fichou, D.; Horowitz, G.; Nishikitani, Y.; Garnier, F. *Chemtronics* **1988**, *3*, 176. (b) Fichou, D.; Horowitz, G.; Nishikitani, Y.; Roncali, J.; Garnier, F. *Synth. Met*. **1989**, *28*, C729. Garnier, F.; Peng, F. Z.; Horowitz, G. *Adv. Mater*. **1990**, *2*, 259.

(4) Akimichi, H.; Waragai, K.; Hotta, S.; Kano, H.; Sakaki, H. *Appl. Phys. Lett*. **1991**, *58*, 1500. Garnier, F.; Yassar, A.; Hajlaoui, R.; Horowitz, G.; Deloffre, D.; Servet, B.; Ries, S.; Alnot, P. *J. Am. Chem. Soc*. **1993**, *115*, 8716.

(5) Katz, H. E.; Dodabalapur, A.; Torsi, L.; Elder, D. *Chem. Mater*. **1995**, *7*, 2238.

(6) Garnier, F.; Yassar, A.; Hajlaoui, R.; Srivastava, P. *Science* **1994**, *265*, 1684.

10.1021/ja053296n CCC: $30.25 © 2005 American Chemical Society

good electron mobilities but very low hole conductivity,[7a] and implemented recently in a carbonyl-functionalized tetrathiophene family.[7b] For these reasons the chemistry of π-conjugated oligothiophenes probably offers the best scenario to study a variety of electrical and optical responses, mostly tunable through judicious modifications of the aromatic π cores and substitution pattern.

An efficient approach to "switch" the oligothiophene conduction mechanism from a p(hole)-channel to n(electron)-channel consists of functionalizing the α- and β-oligothiophene terminal positions with strong electron acceptors. Recently a number of perfluoroalkyl-functionalized oligothiophenes have been synthesized that exhibit very high n-channel field-effect mobilities.[7b−12] This family constitutes suitable n-type counterpart materials of the widely studied p-type alkyl oligothiophenes.[3−6] Equally important, the inclusion of fluoroalkyl chains onto the oligothiophene core enhances substantially molecular thermal stability, volatility, and electron affinity. This family has been investigated targeting mainly the solid-state organization and crystal structures, thin film microstructure and morphology, semiconductor performance, and modeling of the majority charge injection in FET devices.[11,12] However there are a number of fundamental questions related to the electronic structure of these new oligothiophenes and how they relate to the p-type parent systems which need an answer. Such a study, which is the objective of the present paper, provides valuable information for additional structural optimizations of these systems from a molecular level perspective.

Molecular spectroscopy is the fundamental tool to establish structure−property relationships guiding the design of new and improved molecular materials. In particular, Raman spectroscopy is very well suited for the study of conjugated systems. Raman frequencies and intensities are experimental observables emerging directly from the π-conjugated structure which account for the most important electronic signature of oligothiophenes. The effective conjugation coordinate (ECC) model predicts two main trends for the Raman spectra of conjugated molecules: (a) selective enhancement of particular scatterings associated with collective C═C/C−C stretching vibrations of the conjugated path[13] (this phenomenon relates to the occurrence of an electron−phonon mechanism which is at the origin of their outstanding optical and electrical features) and (b) frequency downshift of these intense bands upon relaxation of the skeletal structure as the consequence of either greater π-electron conjugation in the neutral state or quinoidization induced by ionization. When these spectroscopic data are combined with quantum chemical calculations it is possible to assess precisely relevant molecular parameters which would be very difficult to evaluate by conventional experimental techniques. First principles quantum chemical calculations in the framework of DFT theory are very well suited to model extended π-conjugated systems due to implemented electron-correlation effects.

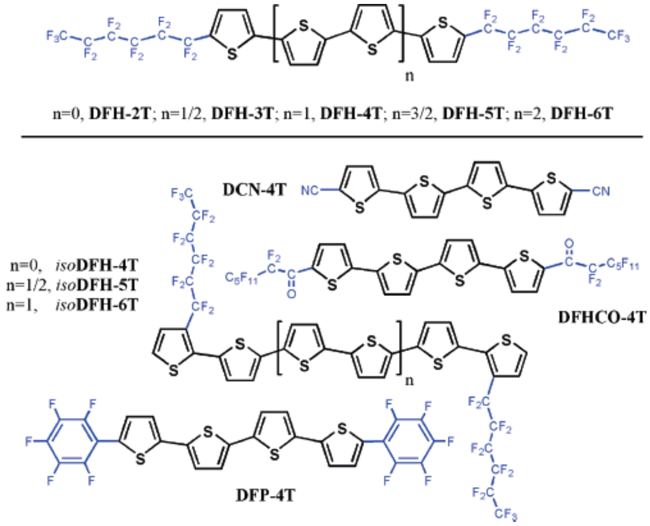

Figure 1. Chemical structures of the molecules studied in this work.

In this contribution Raman spectroscopy and DFT modeling are combined to analyze the molecular and electronic structure of a series of oligothiophenes with variable π−core lengths and substituted at the α,ω- and β,β'-terminal positions with, among others, a variety of perfluorinated groups. The vibrational features of these oligothiophenes are compared to those of the corresponding fluorine-free alkyl- and cyano-substituted systems. The last section of the paper is devoted to understanding the spectral features and molecular structure of the positively charged species, which can provide fundamental information on the molecular properties upon charge injection from the FET contact electrodes.

II. Experimental and Theoretical Details

The syntheses of these oligothiophenes have been published elsewhere.[7−12] Their chemical structures and nomenclature are depicted in Figure 1. Electrochemical oxidation was performed on thin solid films at room temperature in a 0.1 M tetrabutylammonium hexafluorophosphate solution in dry and oxygen-free acetonitrile. Two platinum electrodes were used as auxiliary and working electrodes, and as the pseudoreference a Ag wire was used. Electrolysis conditions were tested against the Fc/Fc$^+$ couple. The procedure consisted of immersion of the film/working electrode in the solution and application of an anodic potential according to the CV data previously recorded in solution. After oxidation proceeds as determined by the color change of the solid, Raman spectra were directly recorded on the coated Pt electrode. The experiments were carried out by using Voltalab40 electrochemical equipment from Radiometer.

FT-Raman spectra were measured using an FT-Raman accessory kit (FRA/106-S) of a Bruker Equinox 55 FT-IR interferometer. A continuous-wave Nd:YAG laser working at 1064 nm was employed for excitation. A germanium detector operating at liquid nitrogen temperature was used. Raman scattering radiation was collected in a backscattering configuration with a standard spectral resolution of 4 cm^{-1}. To avoid possible damage to the oxidized samples upon laser radiation its power was kept to a level lower than 100 mW and 1000−3000 scans were averaged for each spectrum.

---

(7) (a) Chesterfield, R. J.; Newman, C. R.; Pappenfus, T. M.; Ewbank, P. C.; Haukaas, M. H.; Mann, K. R.; Miller, L. L.; Frisbie, C. D. *Adv. Mater.* **2003**, *15*, 1278. Pappenfus, T.; Chesterfield, R. J.; Frisbie, C. D.; Mann, K. R.; Casado, J.; Raff, J. D.; Miller, L. L.; Mann, K. R. *J. Am. Chem. Soc.* **2002**, *124*, 4184. (b) Yoon, M-.H.; DiBenedetto, S. A.; Facchetti, A.; Marks, T. J. *J. Am. Chem. Soc*. **2005**, *127*, 1348.

(8) Facchetti, A.; Deng, Y.; Wang, A.; Koide, Y.; Sirringhaus, H.; Marks, T. J.; Friend, R. H. *Angew. Chem., Int. Ed.* **2000**, *39*, 4547.

(9) Facchetti, A.; Mushrush, M.; Katz, H. E.; Marks, T. J. *Adv. Mater*. **2003**, *15*, 33.

(10) Facchetti, A.; Yoon, M.-H.; Stern, C. L.; Katz, H. E.; Marks, T. J. *Angew. Chem., Int. Ed*. **2003**, *42*, 3900.

(11) Facchetti, A.; Yoon, M.-H.; Stern, C. L.; Hutchison, G. R.; Ratner, M. A.; Marks, T. J. *J. Am. Chem. Soc*. **2004**, *126*, 13480.

(12) Facchetti, A.; Mushrush, M.; Yoon, M.-H.; Hutchison, G. R.; Ratner, M. A.; Marks, T. J. *J. Am. Chem. Soc*. **2004**, *126*, 13859.

(13) Zerbi, G.; Castiglioni, C.; Del Zoppo, M. *Electronic Materials: The Oligomer Approach*; Wiley-VCH: Weinheim, 1998; p 345. Castiglioni, C.; Gussoni, M.; López Navarrete, J. T.; Zerbi, G. *Solid State Commun.* **1988**, *65*, 625.

Density functional theory (DFT) calculations were carried out by means of the Gaussian 98 program[14] running on a SGI Origin 2000 supercomputer. We used Becke's three-parameter exchange functional combined with the LYP correlation functional (B3LYP).[15] It has already been shown that the B3LYP functional yields similar geometries for medium-sized molecules as MP2 calculations do with the same basis sets.[16,17] Moreover, the DFT force fields calculated using B3LYP functional yield vibrational spectra in very good agreement with experiments.[18,19] We also made use of the standard 6-31G** basis set.[20] Optimal geometries were determined on isolated entities in the vacuum. All geometrical parameters were allowed to vary independently apart from planarity of the rings. On the resulting ground-state optimized geometries harmonic vibrational frequencies and Raman intensities were calculated analytically with the B3LYP functional. Calculated harmonic vibrational frequencies are uniformly scaled down by a factor of 0.96 for the 6-31G** calculations, as recommended by Scott and Radom.[18] All quoted theoretical vibrational frequencies reported are thus scaled values. Vertical electronic excitation energies were computed using the time-dependent DFT (TDDFT) approach.[21−24] Radical cations were treated as open-shell systems and computed using spin-unrestricted UB3LYP wave functions. The maximum value obtained for S^2 was nearly 0.77, very close to 0.75 theoretically expected for a doublet, showing that spin contamination is almost absent. Neither solvent effects nor counteranions were considered in the calculations.

III. Experimental and Theoretical Raman Spectra

Analysis of the DFH-*n*T Raman spectra in Figure 2 supports the first statement of ECC theory concerning selective enhancement of rather few lines. Table 1 summarizes the wavenumbers of the most important Raman bands discussed in the paper. For instance, for the largest member of the series, DFH-6T, with more than 300 Raman-active vibrations, only 4−5 lines, in the same frequency range as their shorter parents, are recorded. These bands are markers of the conjugation features and emerge due to the occurrence of an effective electron−phonon coupling. This mechanism qualitatively shows that the pumping (absorption/emission) of optical excitations is regulated by structural or skeletal relaxations by means of phonons or molecular vibrations in the case of van der Waals solids. This effect also accounts for the electron or hole charging/discharging processes inherent to semiconductor charge transport. On one hand its efficiency is at the origin of the Raman intensity since the number of Raman counts in the detector is directly proportional to the number of absorbed photons that are unelastically scattered by a phonon. In addition, the frequencies of these intense Raman lines are related to the molecular reorganization energy after light absorption and unelastic re-emission, which is a key parameter governing charge mobility in organic semiconductors. The vibrations involved in these Raman features mostly correspond to collective C═C stretching modes [ν(C═C)] that mimic the evolution from a heteroaromatic structure (electronic structure of the ground electronic state) to a heteroquinoid structure (electronic structure of the first excited state). The collective character of these vibrations gives rise to a large coupling with the neighboring C−C stretching modes, which are also termed C═C/C−C stretching modes.

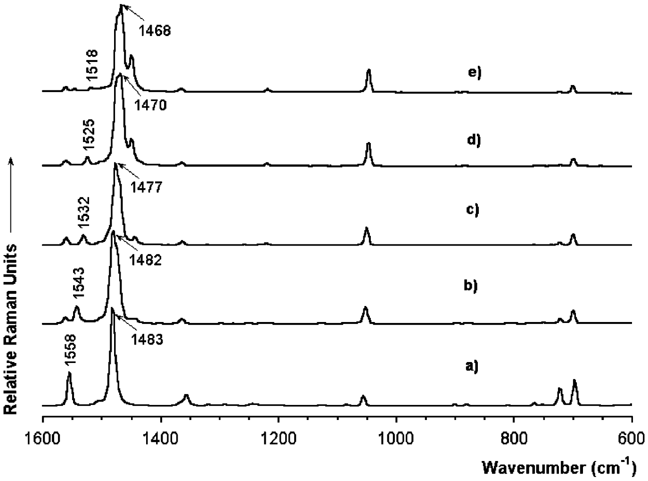

Figure 2. Solid-state FT-Raman spectra of (a) DFH-2T, (b) DFH-3T, (c) DFH-4T, (d) DFH-5T, and (e) DFH-6T. Laser excitation (λ_{exc}) wavelength is 1064 nm.

Figure 3 compares the B3LYP/6-31G** theoretical and solid-state experimental Raman spectra of DFH-4T, while Figure 4 represents some of its normal modes. In general, the theoretical spectrum reproduces the main tendencies of the experimental features even when the scattering spectrum is recorded in solid state. The experimental line at 1532 cm^{-1} is related to that calculated at 1526 cm^{-1} and, according to its eigenvector, is due to a ring antisymmetric ν(C═C) mode with slightly more exterior (terminal rings) character. This band is termed line A and usually shows a large downshift for linear oligothiophenes as a function of the increasing number of thiophene rings, which is an observable of the increment of π-electron conjugation.[25] Line A is measured at 1558 cm^{-1} in DFH-2T, 1543 cm^{-1} in DFH-3T, 1532 cm^{-1} in DFH-4T, 1525 cm^{-1} in DFH-5T, and 1518 cm^{-1} in DFH-6T. As observed, the relative intensity of this line monotonically decreases with the core length increment due to its terminal character.

Line B is the strongest band of the Raman spectrum and in the case of DFH-4T is recorded as a double band component at 1477 and 1472 cm^{-1} that might be related to the two intense computed bands located at 1452 and 1437 cm^{-1}, respectively. These lines are associated with two ν(C═C) modes mainly located at the innermost thiophene rings, which in contrast to line A have a local symmetric character within each ring (see

---

(14) Frisch, M. J. et al.; *Gaussian 98*, Revision A.7; Gaussian, Inc.: Pittsburgh, PA, 1998.

(15) Becke, A. D. *J. Chem. Phys.* **1993**, *98*, 1372.

(16) Stephens, P. J.; Devlin, F. J.; Chabalowski, F. C. F.; Frisch, M. J. *J. Phys. Chem.* **1994**, *98*, 11623.

(17) Novoa, J. J.; Sosa, C. *J. Phys. Chem.* **1995**, *99*, 15837.

(18) Scott, A. P.; Radom, L. *J. Phys. Chem.* **1996**, *100*, 16502.

(19) Rauhut, G.; Pulay, P. *J. Phys. Chem.* **1995**, *99*, 3093.

(20) Francl, M. M.; Pietro, W. J.; Hehre, W. J.; Binkley, J. S.; Gordon, M. S.; Defrees, D. J.; Pople, J. A. *J. Chem. Phys.* **1982**, *77*, 3654.

(21) Runge, E.; Gross, E. K. U. *Phys. Rev. Lett.* **1984**, *52*, 997. Gross, E. K. U.; Kohn, W. *Adv. Quantum Chem* **1990**, *21*, 255. Gross, E. K. U., Driezler, R. M., Eds.; Plenum Press: New York, 1995; p 149.

(22) Casida, M. E. *Recent Advances in Density Functional Methods, Part I*; Chong, D. P., Ed.; World Scientific: Singapore, 1995; p 115.

(23) Koch, W.; Holthausen, M. C. *A Chemist's Guide to Density Functional Theory;* Wiley-VCH: Weinheim, 2000.

(24) The 12 lowest energy electronic excited states were at least computed for all the molecules. The computational cost of TDDFT is roughly comparable to that of single-excitation theories based on an HF ground state, such as single-excitation configuration interactions (CIS). Numerical applications reported so far indicate that the TDDFT formalism employing current exchange-correlation functionals performs significantly better than HF-based single-excitation theories for the low-lying valence excited states of both closed-shell and open-shell molecules.

(25) Hernández, V.; Castiglioni, C.; Del Zoppo, M.; Zerbi, G. *Phys. Rev. B* **1994**, *50*, 9815. Ramírez, F. J.; Hernández, V.; López Navarrete, J. T. *J. Comput. Chem.* **1994**, *15*, 405. Hernández, V.; Casado, J.; Ramírez, F. J.; Zotti, G.; Hotta, S.; López Navarrete, J. T. *J. Chem. Phys.* **1996**, *104*, 9271. Moreno Castro, C.; Ruiz Delgado, M. C.; Hernández, V.; Hotta, S.; Casado, J.; López Navarrete, J. T. *J. Chem. Phys.* **2002**, *116*, 10419. Casado, J.; Katz, H. E.; Hernández, V.; López Navarrete, J. T. *J. Phys. Chem. B* **2002**, *106*, 2488.

Table 1. Lines A and B Wavenumbers (cm^{-1}) for the Most Relevant Compounds

	DFH-2T	DFH-3T	DH-4T	DFH-4T	*iso*DFH-4T	DFP-4T	DFHCO-4T	DCN-4T	DFH-5T	DFH-6T
line A	1558	1543	1537	1532	1532	1518	1516	1516	1525	1518
line B	1483	1482	1487	1477	1471	1460	1456	1447	1470	1468

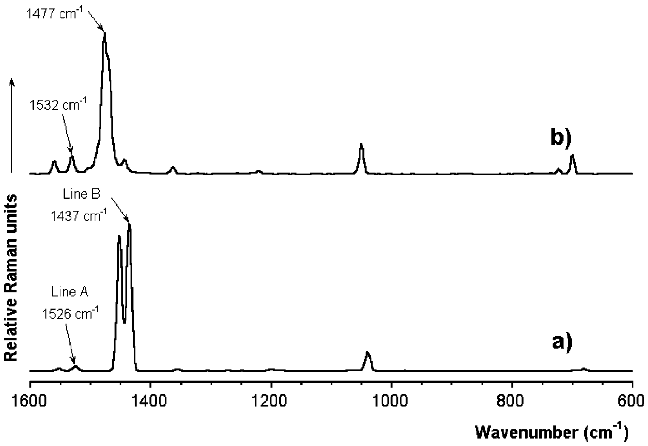

Figure 3. Comparison between (a) theoretical (B3LYP/6-31G**) and (b) experimental solid-state (λ_{exc} = 1064 nm) Raman spectra of DFH-4T.

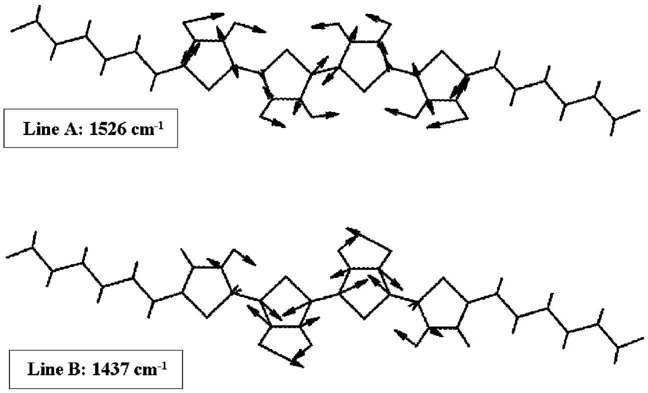

Figure 4. Vibrational eigenvectors associated with the lines at 1526 and 1437 cm^{-1} of the B3LYP/6-31G** Raman spectrum of DFH-4T, lines A and B, respectively.

eigenvector in Figure 4). Line B shows less frequency dependence with chain length but is very sensitive to the electronic alteration of the oligothiophene, i.e., by core oxidation/reduction.[26] When focused on the strongest component, this line is measured at 1483 cm^{-1} in DFH-2T (single component), 1482 cm^{-1} in DFH-3T, 1477 cm^{-1} in DFH-4T, 1470 cm^{-1} in DFH-5T, and 1468 cm^{-1} in DFH-6T. On the lower energy side of line B a new line that increases its intensity on going from the trimer to the hexamer is measured at 1444, 1445, and 1450 cm^{-1} for DFH-3T and DFH-4T, DFH-5T, and DFH-6T, respectively. This line is termed line C and is described as a ν(C=C) vibration always coupled with the dynamic of line B.[25]

Apparently no bands associated with pure atomic motions of the conjugated C−C single bonds (ring or inter-ring ν(C−C) modes) are observed with noticeable intensity since they should appear at 1300 and 1100−1200 cm^{-1}. Only a very weak Raman line at 1364 cm^{-1} (calculated at 1355 cm^{-1}) can be detected and, according to its eigenvector, is associated with a thienyl ring C−C stretching vibration. However, this mode implies some extended C=C movements or coupling, indicating that its dynamics are involved in the already analyzed C=C/C−C stretchings, which reinforces the statement of ECC theory about the collective character of the vibrations associated with the strongest (and observed) spectral features. In agreement with the assignment, this line experiences a maximum shift of 8 cm^{-1} going from DFH-2T to DFH-6T [DFH-2T (1357 cm^{-1}), DFH-3T and DFH-4T (1364 cm^{-1}), DFH-5T and DFH-6T (1365 cm^{-1})] with a concomitant intensity decrease (vide infra, section IV.C).

It is clear that during the C=C/C−C stretching modes the hydrogen atoms of the C−H bonds recoil opposite to the motion of the β-carbons, resulting in a mechanical coupling of the skeletal modes with the in-plane C−H bending modes. The eigenvector of the theoretical band at 1040 cm^{-1} associated with the experimental line at 1051 cm^{-1} for DFH-4T, due to an in-plane β(C−H) mode, exemplifies this fact. The large intensity of this nonskeletal mode must result from this mechanical coupling with the ECC modes.[25]

The pattern of bands from 1000 to 600 cm^{-1} is reproduced nicely by theory. The double doublet of bands at 900−881 and 766−753 cm^{-1} in DFH-2T due, respectively, to the ν(C−S) stretching modes quickly disappears for the longest oligomers due to their local character.[25] However, the 723−698 cm^{-1} doublet, still observed for DFH-6T, corresponds to the in-plane ring deformations, δring, which can certainly be coupled with the ECC modes addressing its detection for the largest system.

IV. Raman Correlations and Electronic Structure: Optical and Electrochemical Analysis

A. Peak Positions of Lines A and B. The first insight of the above discussion is the occurrence of ν(C=C) modes appearing at different wavenumbers according to its physical location in the chain: line A at the outermost rings which peaks around 1520 cm^{-1} and line B at the center which appears around 1475 cm^{-1}. This effect is beyond a mere terminal or boundary effect. Figure 5 depicts the bond distances as deduced from the B3LYP/6-31G** equilibrium geometries for DFH-4T, DH-4T, DM-4T (α,ω-dimethyltetrathiophene), and DCN-4T (α,ω-dicyanotetrathiophene). The averaged distance differences between consecutive CC bonds of the conjugated path defines the BLA parameter,[27] which is positive for aromatic rings, becomes zero for benzene, and inverts the pattern (negative values) for quinoid systems. Hence, a decrease of the BLA pattern of a given thiophene ring can be associated to a decrease of ring aromaticity and increase of quinoid character. This leads to increased linear π conjugation between adjacent thiophenes. It is first noticed that the BLAs for the innermost rings are significantly lower (larger π conjugation or quinoid character) than those of the

---

(26) (a) Casado, J.; Hernández, V.; Hotta, S.; López Navarrete, J. T. *J. Chem. Phys.* **1998**, *109*, 10419. (b) Casado, J.; Hernández, V.; Hotta, S.; López Navarrete, J. T. *Adv. Mater.* **1998**, *10*, 1258. (c) Casado, J.; Miller, L. L.; Mann, K. R.; Pappenfus, T. M.; Kanemitsu, Y.; Ortí, E.; Viruela, P. M.; Pou-Amerigo, P.; Hernández, V.; López Navarrete, J. T. *J. Phys. Chem. B* **2002**, *106*, 3872. (d) Casado, J.; Miller, L. L.; Mann, K. R.; Pappenfus, T. M.; Hernández, V.; López Navarrete, J. T. *J. Phys. Chem. B* **2002**, *106*, 3597.

(27) Brédas, J. L. *J. Chem. Phys.* **1985**, *82*, 3808.

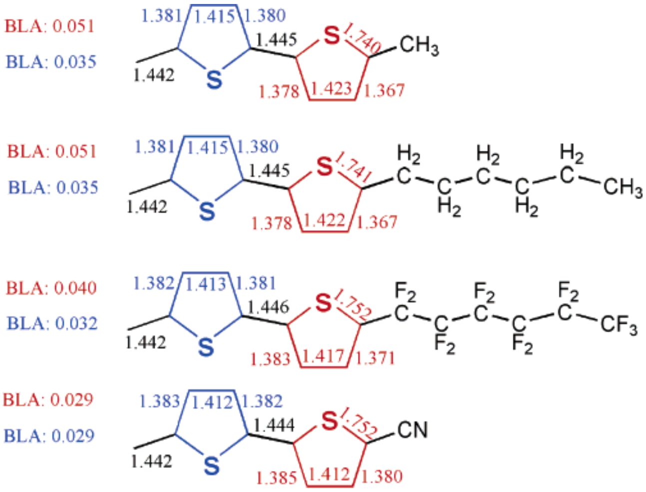

Figure 5. B3LYP/6-31G**-optimized geometries for neutral DM-4T, DH-4T, DFH-4T, and DCN-4T. BLA values are given in Å. Outer and inner rings are in red and blue, respectively.

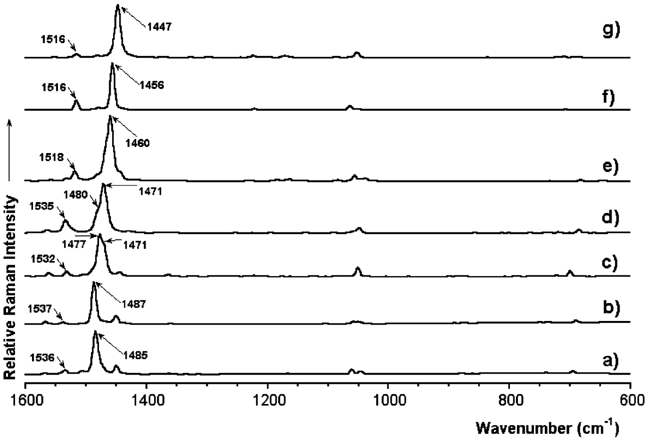

Figure 6. Solid-state FT-Raman spectra of (a) DM-4T, (b) DH-4T, (c) DFH-4T, (d) *iso*DFH-4T, (e) DFP-4T, (f) DCN-4T, and (g) DFHCO-4T. $\lambda_{\text{exc}} = 1064$ nm.

external ones. For instance, the inner/outer BLAs amount to 0.035/0.051, 0.035/0.048, and 0.032/0.040 Å for DM-4T, DH-4T, and DFH-4T, respectively. These structural data support the spectroscopic signatures because line B always appears at lower wavenumbers than line A, according to the ECC argument that a lower Raman wavenumber indicates increased quinoid character.

B. Dependence on α,ω-Terminal Substitution. More structural–spectroscopic correlations can be extracted by comparing the FT-Raman spectra of tetrathiophenes functionalized with electron acceptors of different nature (Figure 6). Spectral lines A and B of DM-4T (1536, 1485 cm^{-1}) and DH-4T (1537, 1487 cm^{-1}) are very similar, in agreement with their identical outer and inner BLAs. However, both lines move toward lower wavenumbers upon fluorination to 1532 and 1477 cm^{-1} (DFH-4T) in accordance with the decrease of both outer (0.051 to 0.040 Å) and inner (0.035 to 0.032 Å) BLAs going from the fluorine-free to the fluorinated oligothiophene.

In the case of DCN-4T the B3LYP/6-31G** outer/inner BLAs are 0.029 Å for both thiophene ring types, in excellent agreement with the much lower peak position of DCN-4T line A (1516 cm^{-1}) and line B (1456 cm^{-1}) relative to those of DFH-4T. Despite the fact that both substituents are strong electron-withdrawing (EWD) groups, the nature of this effect differs substantially. While the perfluorohexyl exhibits a negative σ-inductive effect ($-I$) only, the CN substituent exhibits a weak $-I$ effect but a very strong EWD mesomeric action ($-M$) via thiophene → CN charge transfer. Consequently, the large difference between the wavenumbers of lines A and B and their associated BLAs for DFH-4T and DCN-4T are expected and in agreement with the aforementioned effects. The result of the different EWD substituent action on the thienyl spine has important electronic implications. The cyano group strongly affects the C=C/C–C path of both inner and outer rings, whereas their closer C–S bonds are minimally perturbed (1.752 Å in DFH-4T and DCN-4T), which is an indication that the electron-withdrawal effect is mediated by long-range π interactions. The perfluorohexyl chain, however, perturbs mainly the neighboring C=C (1.367 Å in DH-4T and 1.371 Å in DFH-4T) and C–S (1.741 Å in DH-4T and 1.752 Å in DFH-4T) bonds because its electron-withdrawing effect is mediated by short-range σ interactions.

One beautiful example illustrating the effect of long-range π interactions by means of fluorination can be found in the Raman spectra of DFP-4T and DFHCO-4T where line A appears at 1518 cm^{-1} in the former and 1516 cm^{-1} in the latter, hence largely downshifted with respect to the line A position in DFH-4T but at very similar values to that of DCN-4T. The inclusion of a conjugated spacer (C=O) between the oligothiophene and the fluorinated chain (DFH-4T → DFHCO-4T) has the effect to shift the EWD power from $-I$ to primarily $-M$. The result is a large change in the position of lines A and B: 1537 and 1487 cm^{-1} in DH-4T, 1532 and 1477 cm^{-1} in DFH-4T, 1518 and 1460 cm^{-1} in DFP-4T, 1516 and 1447 cm^{-1} in DFHCO-4T. When the acceptor strength is increased, it appears that electron depletion of the thiophene backbone reaches saturation for the external rings (from DFP-4T to DFHCO-4T line A only changes 2 cm^{-1}) while increases progressively for the more electron-rich central rings (line B changes 14 cm $^{-1}$). The electronic structure changes in the oligothiophenes substituted with $-M$ groups, as outlined by the Raman data, are the consequence of an important drift of electron density from the central π-conjugated backbone toward the π acceptors, which is impossible for σ-only EWD substituents. At the origin of these phenomena lies the existence of an efficient oligothiophene → substituent charge-transfer responsible for most of their optical and electronic properties.

C. Dependence on the Oligothiophene π–Core Length. For the DFH-*n*T series the line A changes are attenuated on going from the shorter to the longer oligomers (15 cm^{-1} from DFH-2T to DFH-3T and 7 cm^{-1} from DFH-5T to DFH-6T), which is in agreement with the BLA attenuation of the outer rings when the core length is increased. On the contrary, line B monotonically decreases with the number of thiophene units (i.e., 5 cm^{-1} from DFH-3T to DFH-4T and 5 cm^{-1} from DFH-5T to DFH-6T), reflecting the progressive structure quinoidization for longer oligomers. One additional structural–spectroscopic correlation is established for the behavior of the ring ν(C–C) stretches that, in contrast to the ν(C=C) modes, increase their wavenumbers upon core lengthening, in agreement with the shortening of these formal single bonds upon quinoidization of the structure or increment of the linear π conjugation between the adjacent rings.

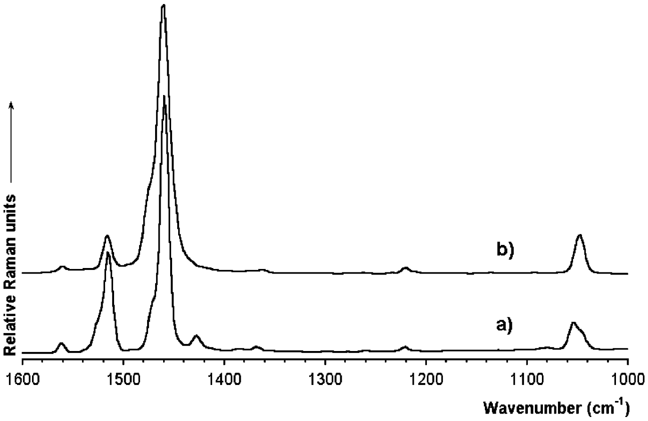

Figure 7. Solid-state FT-Raman spectra of (a) 4T and (b) *iso*DFH-6T. $\lambda_{exc} = 1064$ nm.

D. Dependence on the Regiochemistry of α,*ω*- *to β*,*β*′-*Substitution.* The crystal structures of *β*,*β*′-DFH-disubstituted oligothiophenes (*iso*DFH-nTs), as studied by X-ray diffraction, largely differ from those of their α,*ω*-substituted regioisomers.[11,12] At a molecular level the first important difference between these families is the existence, for the *β*,*β*’-substituted oligothiophenes of *syn*−*anti* configurations involving the two external thiophene rings with respect to the exclusive *all*-*trans* conformation recorded for the α,*ω*-substituted oligomers. Given the terminal character of the line A vibration, its position for *iso*DFH-4T depends minimally on the relative inner ring conformation, and its wavenumber is measured at higher values (1535 cm^{-1}) than those for DFH-4T, proving the mitigation of the electron-withdrawing power for substituents located in the *β* positions. On the other hand, the presence of different conformers in *iso*DFH-*n*Ts does not alter significantly the Raman wavenumbers of line B but only inverts the intensity pattern of its two components: 1477 (stronger) and 1471 cm^{-1} in DFH-4T and 1480 and 1471 cm^{-1} (stronger) in *iso*DFH-4T. It has been shown that the presence of syn/anti conformers in the solid state for a given oligothiophene core length yields changes of line intensity in the Raman spectrum.[28]

The most important structural change upon α,*ω* to *β*,*β*′ *π*−core regiochemical substitution concerns the largest member of the series (6T) and consists of the dramatic increase of the torsional angles between adjacent external thiophene rings compared to the DFH-*n*T series. The magnitude of the torsional angle is larger between the two external rings, 31−64°, versus the internal, 1−30°, core positions,[11,12] although it must be pointed out that the distortions of the inner rings are much more pronounced for the *β*,*β*′ DFH oligomers. Upon realization of this conformational effect one should expect a large influence in the Raman response, as it is nicely illustrated in the next example. Figure 7 displays the Raman spectra of *iso*DFH-6T and unsubstituted tetrathiophene (α4T) which are almost superimposable: the large conformational distortion in *iso*DFH-6T can electronically decouple the two lateral rings with the remaining 4T core resulting in a mean conjugation length similar to that of planar α4T. This electronic picture is also supported by electrochemical data which show that the oxidation (1.20 V) and reduction (−1.81 V) potentials for *iso*DFH-6T are, as a whole, more similar to those of α4T (1.40 and −1.94 V, respectively) than those of DFH-6T (1.06 and −1.42 V). Also, the optical absorption data with maxima at 420 nm for *iso*DFH-6T, 443 nm for DFH-6T, and 391 nm for α4T show that the *β*-substituted compound is halfway between the other two.[11,12] As discussed in the last section, the excited states of *iso*DFH-6T receive very large contributions from quinoid structures which require an extensive planarization of its oligomer backbone. This means that the properties of *iso*DFH-6T (oxidation potentials and absorption data) that increasingly involve these “quinoidal states” will approach the properties of DFH-6T, which is in fact almost planar as observed by X-ray diffraction data.

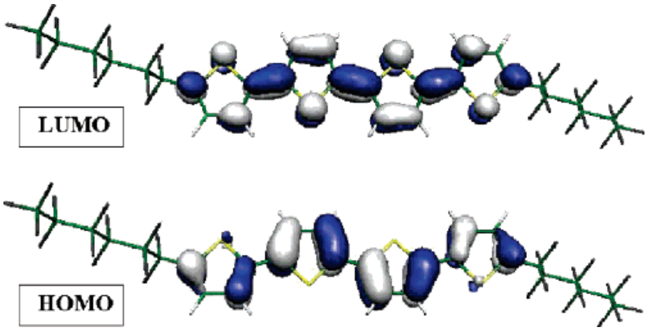

Figure 8. Molecular orbital topologies for the HOMO and LUMO wave functions of DFH-4T.

E. Structural Implications of Line Raman Intensities. The activity of a given Raman line is proportional to changes in the molecular polarizability (α) during the associated vibrational motion. In fact, one of the main terms of the equation for the Raman intensity arises from the dipolar moment transitions, in principle summed over all the electronic states.[29] Consequently, it can be approached that the largest contributions to Raman activity should come from the electronic excitations associated with the most intense band of the electronic spectrum because they, by far, show the largest dipolar moment transitions and oscillator strengths. This band is measured in THF at 4.02 eV ($\epsilon = 17\,500$) in DFH-2T, 3.44 eV ($\epsilon = 28\,900$) in DFH-3T, 3.11 eV ($\epsilon = 39\,000$) in DFH-4T, 2.94 eV ($\epsilon = 40\,200$) in DFH-5T, and 2.78 eV ($\epsilon = 53\,000$) in DFH-6T and corresponds, according to the B3LYP/6-31G** time-dependent DFT calculations carried out for DFH-4T, to an almost monoelectronic excitation from the HOMO to the LUMO orbitals at 2.75 eV and the largest oscillator strength of 1.54. As a result, the most intense Raman lines should be associated with the vibrational modes whose atomic motions mimic the evolution of the aromatic electronic structure from the ground electronic state (related with the HOMO topology) to the quinoid electronic structure of the first excited electronic state (related with the LUMO topology).

The orbital topologies for these two molecular orbitals are depicted in Figure 8. Both *π* orbitals extend over the whole thienyl spine, although the largest atomic coefficients are calculated for the two innermost rings. This reasoning suggests that the greatest contributions to the transition dipole moment between the two terms associated with these frontier orbitals could emerge from dipole reorganizations in the central part of the molecule. Consequently, the Raman lines associated with

---

(28) Muguruma, H.; Saito, T.; Hotta, S. *Thin Solid Films* **2003**, *445*, 26. Ruiz Delgado, M. C.; Casado, J.; Hernández, V.; López Navarrete, J. T.; Fuhrmann, G.; Bäuerle, P. *J. Phys. Chem. B* **2004**, *108*, 3158.

(29) Albrecht, C. A. *J. Chem. Phys.* **1961**, *34*, 1476.

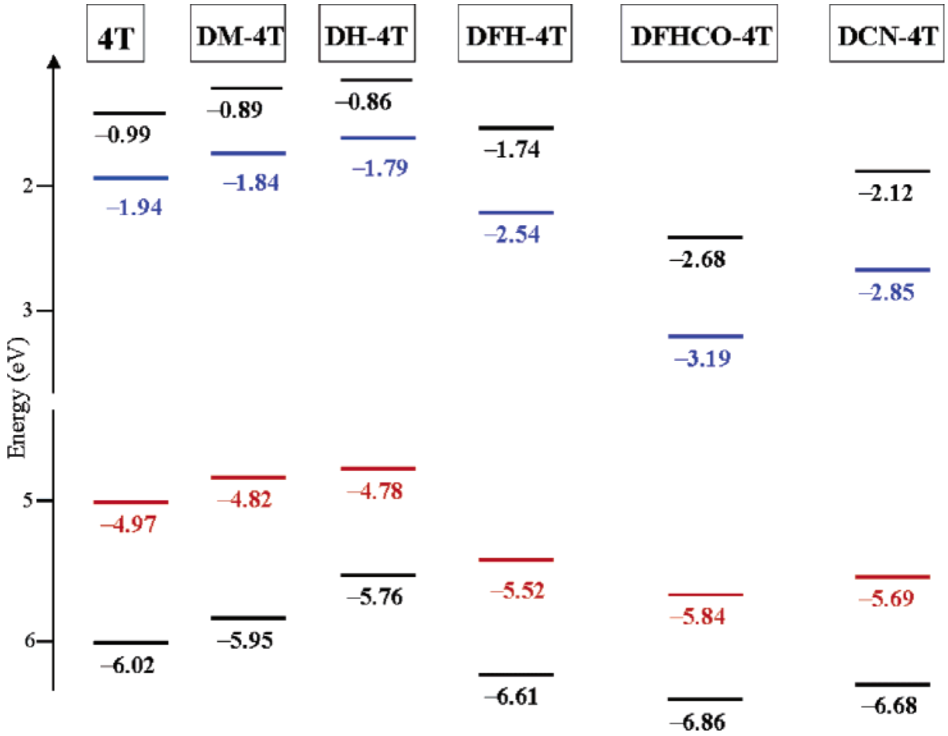

Figure 9. B3LYP/6-31G** one-electron energy diagram including the highest occupied (red) and lowest unoccupied (blue) molecular orbitals.

vibrations located in the central part of the core should exhibit greater intensities. This has been evidenced in the experimental spectra of the oligothiophenes according to the relative intensity of lines A and B.

F. Redox Gap and HOMO/LUMO Energies: Correlations between Raman Spectra and Electronic Structure. Koopman's approach states that the HOMO and LUMO energies relate, respectively, to the ionization potential and electronic affinity, which can be ultimately related to the experimental features associated with the oxidation/reduction potential values.

Furthermore, ambipolar semiconducting behavior in the solid state is primarily determined by the existence of stable oxidation and reduction processes at a molecular level. Figure 9 compares the B3LYP/6-31G** absolute values of the frontier orbitals of the compounds under study. Interestingly, the same tendencies are found for the energy of the frontier orbitals and the peaks of the Raman spectra within the series of compounds. Substitution with $+I$ electron donors slightly increases the energy of both frontier orbitals, and the peak position of line A/B slightly increases (namely, DM4T → DH4T). Furthermore, α,ω-terminal $-I$ substituents give rise to the opposite effect for the orbital energies, and the wavenumber peaks also downshift with the acceptor character. Accounting for these absolute energies, combined electron extraction/injection is greatly facilitated when EWD effects are mediated by π ($-M$) interactions (cyano and carbonyl moieties) and the Raman lines show the most noticeable downshift.

The most relevant comparison is for the most favorable scenario for ambipolar behavior provided by DFHCO-4T, which simultaneously shows the greatest red shift of its Raman spectrum. This discussion is not an accidental coincidence but stresses relevant property−structure relationships. First, in all cases hole/electron interchanges are mediated by the thiophene π-core whose donor/acceptor character is finely tuned by the character of the substituents. These substituents induce an increment of the aromatic character of the thienyl skeleton in the case of electron-donor moieties and favor quinoidization in the case of electron acceptors, with the latter being enhanced for $-M$ EWD groups. As a consequence, it is likely that the ability of a given linear α-oligothiophene to exchange charges with other molecules or metal/conducting polymer electrodes seems to be accounted for by electronic modulation of aromatic/quinoid structures. Hence, an electronic structure suitably balanced by quinoid and aromatic contributions could represent the optimal case to afford ambipolar charge transport in semiconducting organic molecules, and interestingly, Raman spectra through the peak positions of the main bands offer an experimental estimation or measure of this structural balance.

V. Oxidized Oligothiophenes: Raman Spectra and Molecular Structures

This section is devoted to the analysis of the molecular structure based on Raman spectroscopy of the oxidized molecules as prototypical examples of charge injection, which are primarily responsible for the efficiency of the macroscopic transport of charge.

As already discussed, the magnitude of the Raman intensities shows a strong dependence on the transition dipole moment associated with the intensity of the electronic bands. Furthermore, the most important terms of the Raman intensity equation are strongly enhanced when the energy of the laser line used in the experiment coincides with the electronic absorption band; hence, it is stated that resonant Raman conditions are reached.[29] In this case, the scattered intensity associated with a given chromophore can be enhanced by a factor of 10^3-10^6. For this reason, a dependence of the Raman profile of the oxidized oligothiophenes with the laser energy is expected.

Figure 10 displays the FT-Raman spectra of the neutral and singly oxidized DFH-6T. Generation of the radical cation of DFH-6T gives rise to the disappearance of the Raman scatterings

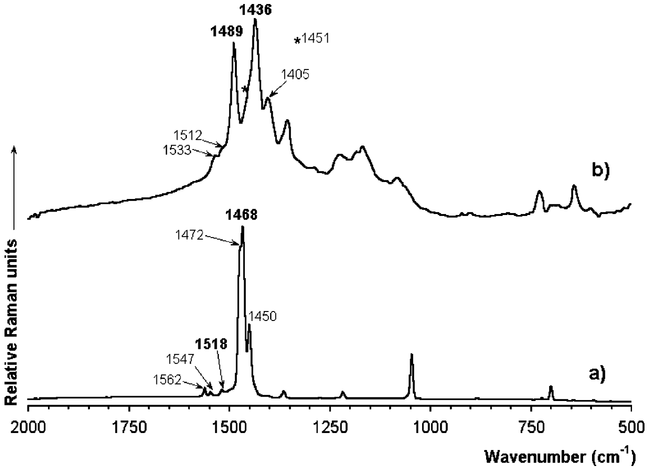

Figure 10. FT-Raman spectra of (a) neutral DFH-6T and (b) electrochemically oxidized DFH-6T$^{\bullet+}$. λ_{exc} = 1064 nm.

of the neutral form and the upsurge of a new set of lines all shifted at low-frequency values according to the following neutral/radical cation correlation in the C═C/C−C stretching wavenumber region: 1562/1533, 1547/1512, 1518/1489, 1472/1451, 1468/1436, and 1450/1405 cm^{-1}. It is possible to relate lines A and B in the spectra of the neutral compound with the corresponding features for the oxidized form at 1489 and 1436 cm^{-1}, respectively. The intensity pattern of singly oxidized DFH-6T is similar to that of the neutral species, although line A is greatly enhanced. The wavenumber change for line B in going from DFH-6T to DFH-6T$^{\bullet+}$ is slightly greater than that of line A, suggesting that the charge defect is mainly accommodated at the central part of the molecule and extends to the outermost rings, which is in agreement with their vibrational topologies. In fact, according to the ECC predictions, the wavenumber downshift of the whole spectrum is consistent with an increased quinoidal character for the singly oxidized oligothiophene. This result is confirmed by theoretical calculations (vide infra).

DFT//(U)B3LYP/6-31G** equilibrium geometries for the neutral and oxidized DFH-6T and *iso*DFH-6T molecules (Figure 11) show that the principal changes upon electron extraction affect the conjugated path. The neutral to radical cation overall BLA value changes from 0.049 to 0.018 (DFH-6T) and 0.053 to 0.020 Å (*iso*DFH-6T) are in agreement with the completely new profile of the Raman spectra of the oxidized species. As accounted for by the BLA data, removal of one electron from the HOMO considerably affects the π system and provokes relaxation of the whole CC skeletal pattern. This softening gives rise to the downward shift of the C═C/C−C stretching Raman lines upon single oxidation. Furthermore, DFT//UB3LYP/6-31G** calculations foresee an evolution from an aromatic to a partially quinoidic pattern, particularly pronounced at the middle of the molecule and progressively decreasing toward the terminal rings (see Figure 11). Quinoidization converts the inter-ring single-bond character of the neutral forms into double-bond character in the doped species, which results in a significant planarization/rigidification of the whole molecular structure.

Figure 12 compares the FT-Raman spectra of the radical cations of DFH-6T and *iso*DFH-6T, which are similar to each other in contrast to the spectra of their neutral forms. Upon oxidation of *iso*DFT-6T one should expect some decrease of the conformational π−core distortions due to partial quinoidization of the backbone; however, this conformational reorganization occurs to such an extent that the spectra of DFH-6T and its β,β'-regioisomer are almost superimposable, in agreement with the similarity between the overall BLA values computed for both radical cations, 0.018 (DFH-6T$^{\bullet+}$) and 0.020 Å (*iso*DFH-6T$^{\bullet+}$). Only a rather small difference of 3 cm^{-1} for line A is observed, 1489 cm^{-1} in DFH-6T$^{\bullet+}$ and 1486 cm^{-1} in *iso*DFH-6T$^{\bullet+}$. Suppose that similar planar structures are achieved for both oligomers in the oxidized states, the greater atomic coefficients in the wave function of the frontier orbitals of the carbon atoms at the α,ω positions versus those at the β,β' suggest a decreased EWD efficiency for the latter fluorinated regioisomers.

Bearing in mind that the EWD effect of the DFH chains and the tendency to delocalize the positive injected charge over the whole thienyl backbone are competitive factors, it follows that quinoidization should extend toward the terminal rings more efficiently in *iso*DFH-6T. In contrast to DFH-4T, where line A is located almost exclusively on the outermost ring at each chain end, for the hexamers line A spreads also over the second ring

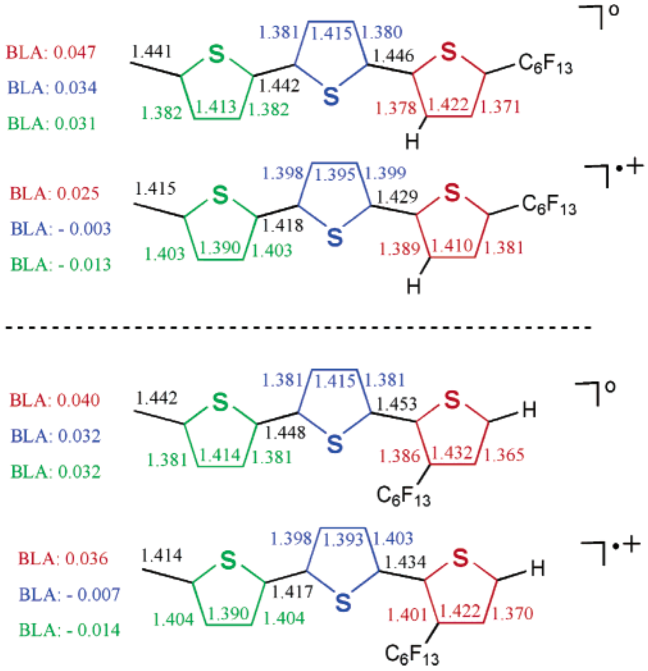

Figure 11. DFT/UB3LYP/6-31G** equilibrium geometries of DFH-6T$^{\bullet+}$ and *iso*DFH-6T$^{\bullet+}$ relative to their neutral homologues.

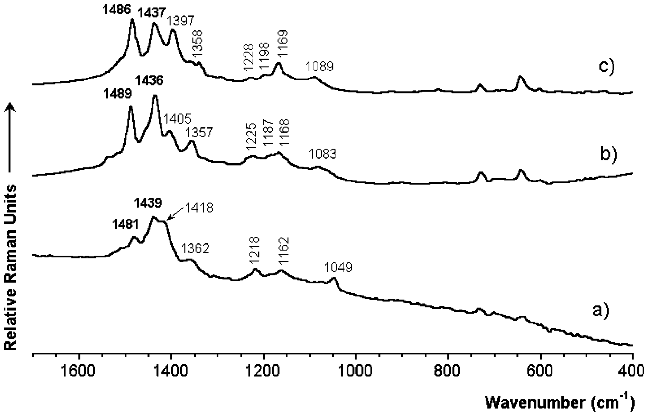

Figure 12. FT-Raman spectra of (a) DH-6T$^{\bullet+}$, (b) DFH-6T$^{\bullet+}$, and (c) *iso*DFH-6T$^{\bullet+}$ electrochemically oxidized thin films. λ_{exc} = 1064 nm.

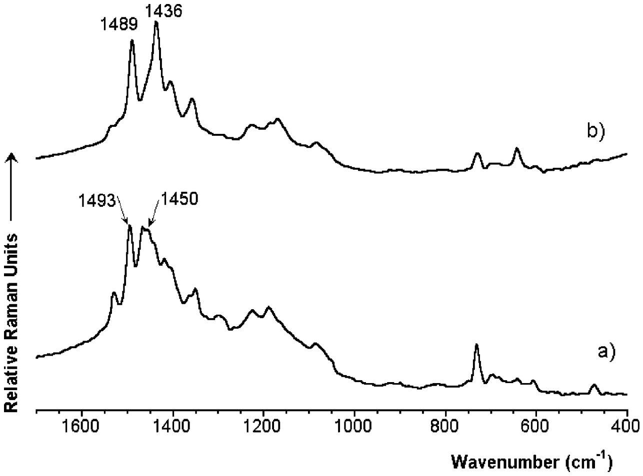

Figure 13. FT-Raman spectra of (a) DFH-5T$^{•+}$ and (b) DFH-6T$^{•+}$ electrochemically oxidized thin films. $\lambda_{exc} = 1064$ nm.

at each end; in fact, the computed BLA value for this second outer ring entirely accounts for the greater quinoidization in *iso*DFH-6T$^{•+}$ (−0.007 Å) than in DFH-6T$^{•+}$ (−0.003 Å) and also for the lower wavenumber of line A in *iso*DFH-6T$^{•+}$. These explanations nicely support the statements outlined in the fourth paragraph of the preceding section about the similarity between the electrochemical and optical properties of DFH-6T and its β,β' regiochemical isomer when "quinoidal states" are taken into account to explain a given spectral/electronic feature.

Oxidation induces further changes in the vibrational spectra (Figure 12); thus, for the DFH-6T/DH-6T radical cations line A appears at 1489/1481 cm^{-1} while line B is measured at 1436/1439 cm^{-1}. The electron-withdrawal effect of the fluorinated chains, greater over the α,ω-terminal positions, impedes the positive charge expansion toward them, so that line A appears at higher wavenumber values (namely, lower quinoidal character) in the case of DFH-6T. For the same reason the positive charge is highly concentrated in the center (slightly increased quinoidal character) and line B downshifts (1436 cm^{-1}) in DFH-6T compared to its fluorine-free parent (1439 cm^{-1}).

It is commonly found for linear oxidized quinquethiophenes to absorb radiation around 1100 nm, always at lower wavelengths than the hexamers. It is therefore reasonable to think that their FT-Raman spectra are influenced by resonance effects (namely, a Nd:YAG $\lambda_{exc} = 1064$ nm is commonly used). The spectrum of the radical cation of DFH-5T, in Figure 13, shows that the strongest lines appear at 1493 and 1450 cm^{-1}, therefore upshifted with respect to its hexamer parent. This observation agrees with what was observed in going from neutral DFH-6T to neutral DFH-5T, where the wavenumber of the strongest Raman line increases. Hence, in this case, $\pi-$core contraction greatly confines the charge defect, resulting in a more marked quinoidic structures and a higher wavenumber for its associated Raman lines.

VI. Conclusions

Correlations between molecular parameters and Raman wavenumbers and intensities have been reported for a series of oligothiophenes, which provide a new perspective and knowledge of the electronic structure of the oligothiophene family regarding the type of substituent (namely, with ± inductive/mesomeric effects), regiochemistry, oxidation state, etc. This study has been carried out primarily on a new fluorocarbon-functionalized oligothiophene series whose technological importance for application of organic semiconductors in the field of molecular electronics is already established. The study has been guided, first, by the assignment of Raman lines with the help of density functional calculations and within the framework of the ECC theory that allows realization of the key bands, lines A and B, involved in π conjugation. Importantly, the collective character of the key ECC vibrations and the molecular frontier orbital wave functions (HOMO and LUMO) primarily determine the electronic properties of the DFH-*n*T oligothiophene series (namely, vibrational Raman and optical spectra, electrochemical, solid-state properties, etc.) In this sense, perfluoroalkylation of the terminal positions finely tunes $\pi-$core properties.

The dependence of the BLA parameter on the oligothiophene $\pi-$core extension and substitution pattern is in agreement with Raman spectra line assignment. Furthermore, the analysis of the Raman lines has been correlated with the σ- ($-I$) and π-mediated mesomeric ($-M$) EWD substituent effects over the thienyl skeleton. The concept of mean conjugation length has been successfully used to compare the vibrational and electronic features of DFH-*n*T and *iso*DFH-*n*T series.

The electrochemically charged DFH-*n*T/*iso*DFH-*n*T films species have been also investigated. The analysis has been focused on the oxidized species, and more work is presently in progress regarding the reduced forms since they are not stable on the time of the Raman experiment. By now the study of positively charged species has proved suitable to monitor the effect of charging/discharging on the electronic structure of these oligothiophenes. In this sense careful analysis of line A and B peak positions has served to address the degree of quinoidization of the charged species, which is again strongly influenced by the substituent regiochemical arrangement and core extension. To summarize, this paper provides a useful approach based on Raman spectroscopy and DFT quantum chemistry to investigate the molecular and electronic properties of fundamental oligothiophenes, which could be extended to any other conjugated material series. This conclusion satisfies the general scope exposed in the Introduction about the possibility of analyzing at a molecular level with reliable accuracy the molecular properties of this ever-growing important class of modern organic materials.

Acknowledgment. J.C. is grateful to the Ministerio de Ciencia y Tecnología (MCyT) of Spain for a Ramón y Cajal research position of Chemistry at the University of Málaga. The present work was supported in part by the Dirección General de Enseñanza Superior (DGES, MEC, Spain) through research project BQU2003-03194. We are also indebted to Junta de Andalucía (Spain) for funding our research group (FQM-0159). The Northwestern group thanks ONR (N00014-02-1-0909), the NSF-MRSEC program through the Northwestern Materials Research Center (DMR-0076097), and the NASA Institute for Nanoelectronics and Computing (NCC 2-3163) for support. We also thank Myung-Han Yoon for providing a sample of DFHCO-4T.

Supporting Information Available: Reference 14 is provided. This material is available free of charge via Internet at http://pubs.acs.org.

JA053296N